agriculture

MDPI

Article

Transmission Characteristics and Experiment of Hydraulic–Mechanical Transmission of Cotton Picker

Huajun Chen [1,†], Meng Wang [1,2,†], Xiangdong Ni [1,*], Xiangchao Meng [1], Wenqing Cai [3], Yiqing Li [1], Baoyu Zhai [1], Hongbin He [1] and Yuyang Wang [4]

[1] College of Mechanical and Electrical Engineering, Shihezi University, Shihezi 832003, China; chenhuajun@stu.shzu.edu.cn (H.C.); wangmeng@shzu.edu.cn (M.W.); mengxiangchao@stu.shzu.edu.cn (X.M.); liyiqing@stu.shzu.edu.cn (Y.L.); zhaibaoyu@stu.shzu.edu.cn (B.Z.); hehongbin@stu.shzu.edu.cn (H.H.)
[2] Key Laboratory of Modern Agricultural Machinery, Xinjiang Production and Construction Corps, Shihezi 832003, China
[3] College of Information Science and Technology, Shihezi University, Shihezi 832003, China; cwq0526@sohu.com
[4] School of Traffic and Transportation, Beijing Jiaotong University, Beijing 100044, China; 22251054@bjtu.edu.cn
* Correspondence: nxd_mac@shzu.edu.cn
† These authors contributed equally to this work.

Abstract: To overcome the issue of unstable speed output encountered by cotton pickers operating in harsh environments and subject to frequent external load fluctuations, a hydraulic–mechanical transmission (HMT) for cotton pickers is proposed in this study. By analyzing the driving system of the cotton picker, a Lavira-based HMT scheme is developed. The matching characteristics of the HMT speed ratio are analyzed, a continuity and smoothness test of the speed ratio of the changing segment is carried out, and the influence law of smoothness of the HMT changing segment is discussed. The results show that the HMT system effectively satisfies the driving speed requirements for both field harvesting and road transportation of cotton pickers. The HMT speed ratio is continuously controllable and the design is reasonable. The HMT load torque and the oil pressure in the main oil circuit have a significant impact on the smoothness indicators of speed reduction and dynamic load. Additionally, the flow rate of the governor valve has a notable effect on the smoothness indicator of sliding friction power. However, the engine's output speed has no significant influence on the HMT's smoothness. This research can provide theoretical support for the development and design of cotton picker gearboxes and the transmission characteristics and experimental research of off-road vehicle gearboxes.

Keywords: cotton picker; hydraulic–mechanical transmission; transmission characteristic; experiment; shift smoothness

Citation: Chen, H.; Wang, M.; Ni, X.; Meng, X.; Cai, W.; Li, Y.; Zhai, B.; He, H.; Wang, Y. Transmission Characteristics and Experiment of Hydraulic–Mechanical Transmission of Cotton Picker. *Agriculture* **2024**, *14*, 1250. https://doi.org/10.3390/agriculture14081250

Academic Editor: Fengwei Gu

Received: 15 June 2024
Revised: 16 July 2024
Accepted: 24 July 2024
Published: 29 July 2024

1. Introduction

Cotton plays an important role in Xinjiang's economic development and social stability, and has an important strategic position [1–3]. In the process of cotton production, picking is an indispensable link, and machine picking is an important guarantee for improving the quality of the cotton industry [4–6]. The operating environment of the cotton picker is harsh, with frequent and wide fluctuations in external load. It works under high load for a long time within the operating conditions, with high power transmission and low speed. During transportation, the load is small and the driving speed is fast. [7,8]. This requires the transmission of the drive system of the cotton picker to be able to change the speed and torque under harsh working conditions in a timely manner to adapt to the constant change in the actual load [9,10].

Hydraulic–mechanical transmission (HMT) effectively combines the characteristics of step-less speed regulation and the fast response of hydraulic transmission with the high

efficiency and high reliability of mechanical transmission [11]. And it can adapt to harsh working environments, and has been widely applied to engineering vehicles, military vehicles, and agricultural vehicles [12–14]. Young-Jun Park et al. developed a hydraulic–mechanical transmission (HMT) model for tractors, subsequently analyzing the power transmission characteristics of tractors equipped with HMT [15,16]. The study confirms the capability of the main shift to split and cycle power in accordance with the motion mode of the static pressure unit, contributing to the optimization of power distribution within the transmission system. Ahn, H.-J. conducted a detailed analysis of the power requirements for agricultural tractors with three distinct power outputs: 78 kW, 80 kW, and 120 kW [17–19]. Their research includes field tests on the main power source shaft, energy pumping device, main hydraulic pump, and auxiliary hydraulic pump, providing valuable insights into the practical application of HMT systems in agricultural machinery. İnce, E. has since advanced the field by developing a novel power distribution input coupled with an IVT system [20]. This development has allowed for the study of the influence of various dynamic parameters on the mechanical efficiency of the system, thereby further refining the understanding and optimization of HMT systems for agricultural applications.

Currently, hydraulic–mechanical transmission is widely used in cotton pickers [21–23]. Chen Wanqiang proposed a design scheme of a step-less transmission of a cotton picker based on the principle of hydraulic power distribution and analyzed its transmission characteristics [24,25]. Bao Mingxi et al. conducted an in-depth study on the coupling characteristics of the hydraulic–mechanical continuously variable transmission of the cotton picker through the test bench, providing a reference for the design of the shift smoothness of the cotton picker [26,27]. Zhong Chunfa proposed a driving scheme of step-less speed regulation by combining hydrostatic step-less speed transmission with mechanical step-less speed transmission, as well as step-less speed regulation during the whole operation, to meet its driving power requirements [28]. Their research proposed the design of cotton picker gearboxes that are hydraulically coupled single-row planetary wheel gearboxes, but due to the lack of alternating redundant planetary rows with opposite speed characteristics to complete the speed articulation, the difficulty of controlling the impact of the changeover is higher than that of the multi-planet row speed control system.

In this study, a Ravigneaux-type HMT design for a 4MZD-6 cotton picker is proposed. Based on the analysis of the HMT characteristics of cotton pickers, it is proposed to conduct tests on the continuity and smoothness of HMT speed ratio matching, which is designed to further validate the feasibility and rationality of the transmission design scheme and to explore the influencing factors of HMT gear change smoothness. The findings lay the groundwork for optimizing the design, testing, and control of cotton picker gearboxes and offer a reference for the study of the reliability of cotton pickers and other engineering vehicles.

2. Materials and Methods

2.1. Cotton Picker Driving System and Travelling Parameters

The main characteristic parameters of the driving system of different pickers are shown in Table 1, which shows that different cotton pickers' driving speed ranges are roughly the same, with picking speed up to 9 km/h, and transport speed up to 32.2 km/h.

Table 1. Main characteristic parameters of cotton picker driving system.

Brand	**CRCHI** [1]	**SSCIM** [2]	**John Deere**		**Case**
Type	**4MZD-6**	**4MZD-6**	**CP690**	**CP770**	**CE 635**
Engine rated power (kW)	570	566	418	414	298
Initial picking maximum speed (km/h)	7.1	7.1	7.1	7.4	6.8
Repeat picking Maximum speed (km/h)	8.5	8.5	8.5	9	7.9
Transportation maximum speed (km/h)	27	27	27.4	32.2	24.1

[1] China Railway Construction Heavy Industry Co., Ltd., Zhuzhou, China. [2] Shandong Swan Cotton Industrial Machinery Co., Ltd., Jinan, China.

2.2. Cotton Picker Hydro-Mechanical Gearbox Transmission Program

In alignment with the prevalent transmission specifications for cotton pickers, the present research independently constructs a transmission program. This program introduces a novel hydraulic–mechanical transmission (HMT) design for cotton pickers, which integrates a "variable pump + variable motor" configuration with a Lavina-type planetary gear mechanism to achieve torque convergence. On the basis of the original HMCVT design, in order to reduce the number of clutches and brakes and further reduce the number of gears, we put forward the HMT design. The design is tailored to a specified speed spectrum, with a low-speed gear range of 0 to 9 km/h and a high-speed gear range of 9 to 27 km/h, adhering to the isometric transmission rule of variation. The HMT scheme principle is shown in Figure 1. HMT divides the engine power into mechanical and hydraulic circuits. Hydraulic components mainly include variable pumps and variable motors, and mechanical components include fixed shaft gears (i_1, i_2), bidirectional clutches (C1 and C2), forward gears (i_3), and reverse gears (i_4). The Lavina-type planetary wheel system constitutes the convergence mechanism of the HMT, where the mechanical and hydraulic power flows are harmonized and subsequently transferred to the output shaft.

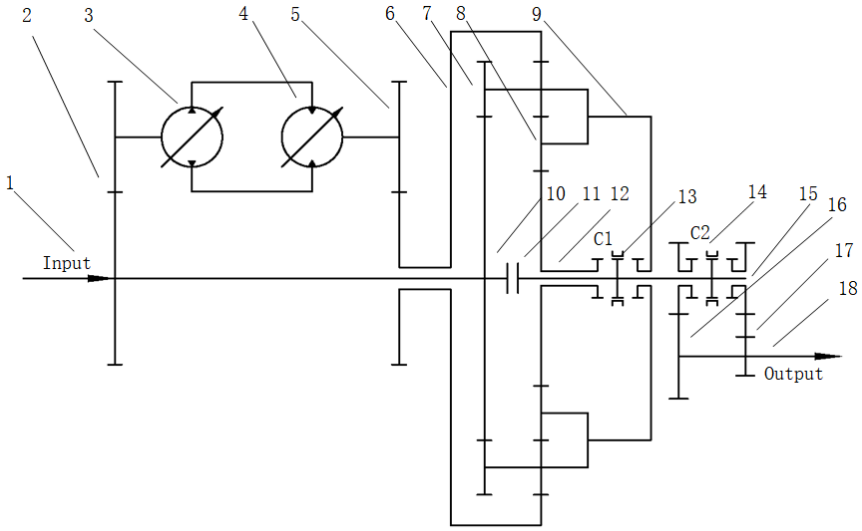

Figure 1. HMT principle diagram. 1—engine input shaft; 2—gear pair i_1; 3—variable pump; 4—variable motor; 5—gear pair i_2; 6—gear ring; 7—long planetary wheel; 8—short planetary wheel; 9—planet carrier; 10—sun wheel 1; 11—coupling; 12—sun wheel 2; 13—bidirectional clutch C1; 14—bidirectional clutch C2; 15—intermediate shaft; 16—forward gear pair i_3; 17—reverse gear pair i_4; 18—output shaft.

2.3. HMT Ratio Matching

2.3.1. Logic of Changing Segments in Each Zone

As can be seen from Figure 1, bidirectional clutches C1 and C2 control the HMT working mode of the cotton picker and are used to change the power transmission route. Different from the traditional clutch, the bidirectional clutch can replace two ordinary clutches while realizing the combination of one side of the power and the other side of the power to disconnect, saving installation space and improving the control accuracy, the control of the HMT change section logic as shown in Table 2, and the low-speed section of the *HM1* section and the high-speed section of the *HM2* section of the power transmission path, as shown in Figure 2. The difference between working forward and working backward is that the transmission ratio of the output end shown in Figure 2 and the clutch engagement state shown in Table 2 are not the same.

Table 2. Clutch manipulation logic for each work zone of HMT.

Working Condition	Segment	Clutch Serial Number and Status	
		C1	C2
Forward	*HM1*	Right engagement	Left engagement
	HM2	Left engagement	Right engagement
Backward	*HM1*	Right engagement	Right engagement

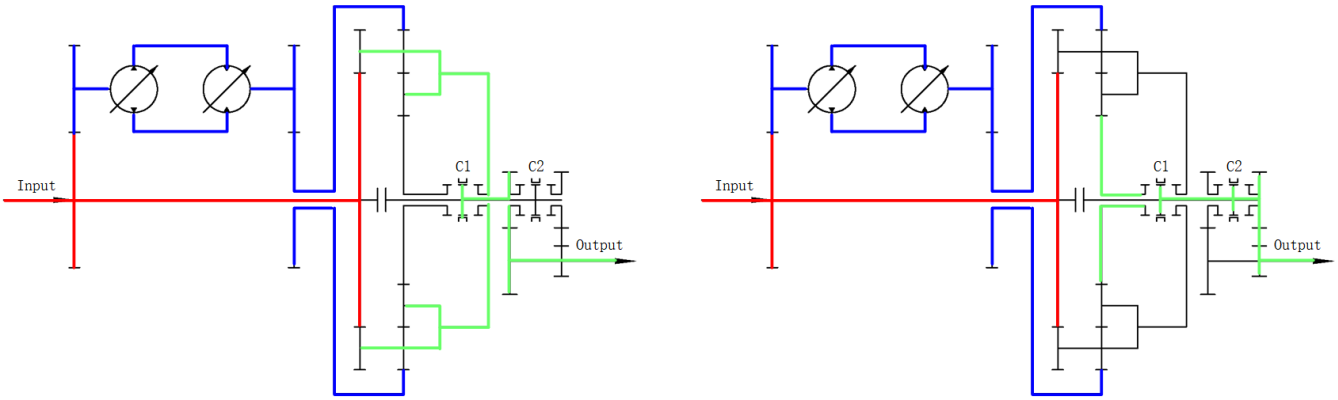

(**a**) *HM1* section (**b**) *HM2* section

Figure 2. Power transmission routes for HMT segments. The blue thick solid line represents the hydraulic power flow, the red thick solid line represents the mechanical power flow, and the green thick solid line represents the output power flow after the convergence of the Lavina-type planetary gear mechanism.

2.3.2. HMT Speed Ratio Parameter Matching

The HMT in this study is mainly adapted to self-propelled cotton pickers and other off-road vehicles, which must simultaneously meet the vehicle field operation walking and inter-area operation road transportation speed requirements. For the design of HMT equipped with cotton picker operating speed with the SSCIM parameters in Table 1, the standard Lavina planetary wheel system speed must meet the following relationship:

$$\begin{cases} n_{s1} + k_1 n_{R1} - (1 + k_1) n_{C1} = 0 \\ n_{S2} - k_2 n_{R2} - (1 - k_2) n_{C2} = 0 \\ n_{C1} = n_{C2} \\ n_{R1} = n_{R2} \\ k_1 < k_2 \end{cases} \quad (1)$$

In Formula (1), n_{s1} is the rotation speed of the large sun wheel, rpm; n_{s2} is the rotation speed of the small sun wheel, rpm; n_{R1} and n_{R2} are the rotation speed of the gear ring, rpm; n_{C1} and n_{C2} are the rotation speed of the planetary carrier, rpm; and k_1 and k_2 are the characteristic parameters of the planetary rows [13].

In the closed hydraulic circuit, the relationship between the variable motor and variable pump is as follows:

$$n_m = n_p \varepsilon \quad (2)$$

In Formula (2), n_p is the input shaft speed of the variable pump, rpm; n_m is the output shaft speed of the variable motor, rpm; ε is the displacement ratio of the pump-controlled hydraulic motor.

The relationship between the transmission ratio and vehicle traveling speed is as follows:

$$\begin{cases} i_k = \frac{\omega_1}{\omega_2 i_r i_w} \\ \omega_1 = \frac{2\pi n_0}{60} \\ \omega_2 = \frac{3600v}{1000r_d} \end{cases} \quad (3)$$

In Formula (3), i_k is the total transmission ratio; ω_1 is the engine speed, rad/s; ω_2 is the wheel speed, rad/s; n_0 is the engine speed, rpm; v is the vehicle's traveling speed, km/h; r_d is the equivalent radius of the driving wheels, m; i_r is the rear axle main deceleration ratio; and i_w is the vehicle's wheel side deceleration ratio. This can be simplified to obtain

$$i_k = 0.377\frac{n_0 r_d}{v i_r i_w} \quad (4)$$

The ratios of the gearbox segments are deduced to be

$$\begin{cases} i_{HM1} = \frac{i_1 i_2 (1+k_1)}{i_1 i_2 + \varepsilon k_1} \\ i_{HM2} = \frac{i_1 i_2 (1+k_1)}{\varepsilon k_2 (1+k_1) + (1-k_2)(i_1 i_2 + \varepsilon k_1)} \end{cases} \quad (5)$$

In Formula (5), i_{HM1} and i_{HM2} are the transmission ratios of the gearbox in the *HM1* section and the gearbox in the *HM2* section, respectively.

According to the design scheme, n_0 = 2400, i_r = 3.7, i_w = 5.6, and r_d = 0.858 are substituted into Formula (4) to obtain the range of ratios for each segment of the gearbox: i_{HM1} ϵ (6.25,2.08) and i_{HM2} ϵ (2.08,0.69). When $\varepsilon = 1$, i_{HM1} and i_{HM2} take the limiting value of 2.08. When $\varepsilon = -1$, i_{HM1} and i_{HM2} take the limiting values of 6.25 and 0.69, respectively. Considering that the value of the planetary row characteristic parameter k is in the range of 1 to 4, $k_1 = 2$, $k_2 = 4$, $i_1 i_2 = 4$, $i_3 = 2$, and $i_4 = -2$ can satisfy the gearbox's speed ratio change and synchronous segment change demand.

From Equation (4), the total transmission ratio of the vehicle is 141.34 when the driving speed of the adapted vehicle is 25 km/h; the total transmission ratio of the vehicle is 28.27 km/h when the driving speed is 5 km/h.

2.4. Characterization of HMT Speed Ratio Matching

2.4.1. Transmission Ratio with Displacement Ratio Change Characteristics

According to the logic of the cotton picker HMT section change, when the cotton picker is in the forward operation *HM1* section, the HMT starts up, and the pump displacement ratio ε changes smoothly from 0 to −1. After the start-up, it enters the acceleration state, with the pump displacement ratio ε transitioning smoothly from −1 to 1. When the cotton picker's HMT accelerates to the highest output speed in the low-speed segment of the *HM1* section, the bi-directional clutch C1 and C2 are engaged, and the HMT shifts to the forward operation *HM2* section, with the pump displacement ratio ε changing smoothly from 1 to −1. The astern working condition is the same as that of the *HM1* section, and the transmission ratio variation characteristics of each section of HMT are shown in Table 3.

Table 3. The character of transmission ratio of each section of HMT with displacement ratio.

Segment	*HM1*	*HM2*
Forward working condition	$i_{HM1} = \frac{12}{4+2\varepsilon}$	$i_{HM2} = \frac{12}{12-6\varepsilon}$
Backward working condition	$i_{HM1} = -\frac{12}{4+2\varepsilon}$	----

According to Table 3, the ratio characteristic curve of each HMT zone can be drawn, as shown in Figure 3. From Figure 3, it can be seen that the speed ratio of each section of HMT varies continuously and smoothly with the pump displacement ratio ε. The output speed of HMT can be accurately controlled by adjusting the HMT pump displacement ratio ε. Its

maneuvering characteristics are good, and the walking system of the cotton picker has the ideal forward speed and backward speed.

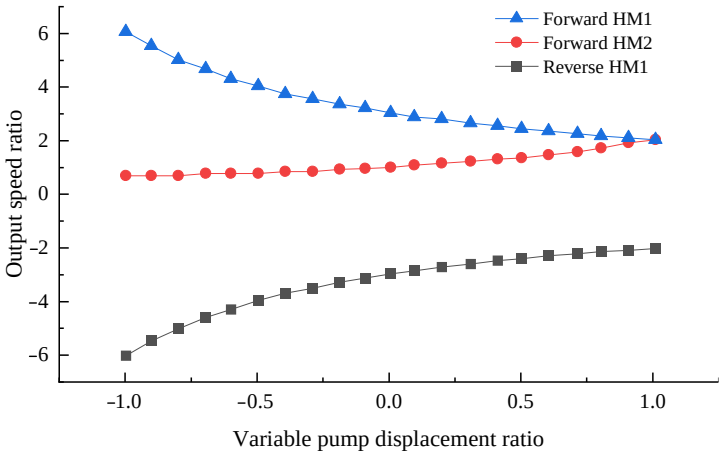

Figure 3. The characteristic of the transmission ratio of each section of HMT with the displacement ratio.

2.4.2. Driving Speed with Displacement Ratio Change Characteristic Analysis

The cotton picker HMT supporting engine rated speed is 2400 r/min; the diameter of the supporting drive wheel is 1685 mm. The cotton picker driving speed characteristic curve can be drawn according to the HMT sections of the transmission ratio formula, as shown in Figure 4.

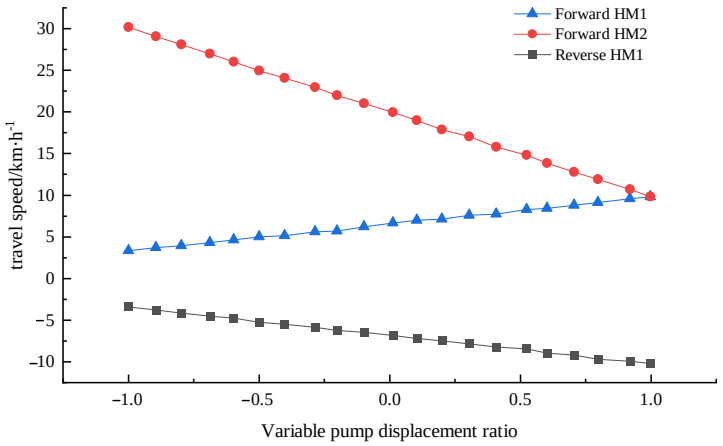

Figure 4. Traveling speed of cotton picker at engine speed 2400 r/min.

Analysis of Figure 4 indicates that under rated operating conditions, the designed HMT program for the cotton picker is feasible for continuously and uniformly adjusting the travel speed during operation. The cotton picker's speed adjustment range is 3–10 km/h in both the low-speed forward section and low-speed backward section of *HM1*, and 10–30 km/h in the forward section of *HM2*, which meets the requirements for the travel speed of the cotton picker in both field harvesting and highway transportation states.

2.4.3. Torque Characterization

The relationship between the HMT output torque and the motor torque is called the HMT torque characteristic, and the torque suffered by the planetary gear structure

sun wheel, planetary wheel, and planetary carrier satisfies the following characteristic equations [15]:

$$\frac{M_s}{-1} = \frac{M_r}{-k\eta_o^\beta} = \frac{M_c}{1+k\eta_o^\beta} \tag{6}$$

In Formula (6), M_s is the torque applied to the sun wheel, N·m; M_r is the torque applied to the planetary wheel, N·m; M_c is the torque applied to the planetary carrier, N·m; η_0 is the converting mechanism mesh efficiency; and β is the converting mechanism mesh power flow exponent. When M_s $\omega_s > 0$, the sun wheel is the active member in the conversion mechanism, and the value of β is -1 at this time. When $M_s\omega_s < 0$, the gear ring is the active member in the conversion mechanism, and the value of β is +1 at this time [21].

The following can be obtained from Formula (6):

$$\begin{cases} M_s k\eta_0^\beta - M_r = 0 \\ M_s(1+k\eta_0^\beta) + M_c = 0 \\ M_r(1+k\eta_0^\beta) + k\eta_0^\beta M_c = 0 \end{cases} \tag{7}$$

The converting meshing efficiency η_0 can be expressed by the product of the meshing efficiency η_1 of the solar wheel and the planetary wheel and the meshing efficiency η_2 of the planetary wheel and the gear ring:

$$\eta_0 = \eta_1\eta_2 \tag{8}$$

In Formula (8), η_1 is the sun wheel and short planetary wheel engagement efficiency; η_2 is the sun wheel and short planetary wheel engagement efficiency; η_3 is the long planetary wheel and short planetary wheel engagement efficiency.

In a single-row double-planetary-gear mechanism, the external forces acting on the basic members of the planetary wheel train satisfy the following relational equation:

$$\frac{M_s}{-1} = \frac{M_r}{k\eta_{oc}^\beta} = \frac{M_c}{1-k\eta_{oc}^\beta} \tag{9}$$

From Formula (9), we can infer the following:

$$\begin{cases} M_s k\eta_{oc}^\beta + M_r = 0 \\ M_s(1-k\eta_{oc}^\beta) + M_c = 0 \\ M_r(1-k\eta_{oc}^\beta) - k\eta_{oc}^\beta M_c = 0 \end{cases} \tag{10}$$

Among them,

$$\eta_{oc} = \eta_1\eta_2\eta_3 \tag{11}$$

At the low-speed section *HM1*, the cotton picker HMT torque characteristic model is established, and the torque characteristics of its gear ring (6) and planetary carrier (9) are

$$\begin{cases} M_6 = M_m i_2 \\ M_9 = \frac{M_6(1-k\eta_{0H}^\beta)}{k\eta_{0H}^\beta} \end{cases} \tag{12}$$

At the high-speed section *HM2*, the toothed ring speed is input from the motor, and the torque is output from sun wheel 2. Similarly, the torque characteristic equations for the toothed ring (6) and sun wheel 2 (12) can be obtained:

$$\begin{cases} M_6 = M_m i_2 \\ M_{12} = -\frac{M_6}{k\eta_{0H}^\beta} \end{cases} \tag{13}$$

From Formula (13), when the motor displacement is constant, the closed hydraulic circuit has constant torque output characteristics, the output torque of the hydraulic power-shunt CVT is constant in each zone, and the ratio of the output torque to the motor torque of the HMT in the *HM1* and *HM2* zones is 1.5 and 0.5, respectively.

2.4.4. Characteristic Analysis of Hydraulic Power Shunt Ratio

The hydraulic power shunt ratio ρ is an evaluation index of the power characteristics of the cotton picker HMT, which is expressed as the ratio of the shunted hydraulic circuit power P_m to the total output power P_{HMi} of the HMT [26], shown in Formula (14). Due to the leakage in the closed hydraulic circuit, the smaller the ratio of the hydraulic circuit power to the total output power of the HMT, the higher the HMT efficiency.

$$\rho = \frac{p_m}{p_{HMi}} \tag{14}$$

The HMT power characteristics were modeled for the low-speed section of the cotton picker during the *HM1* forward section:

$$\begin{cases} P_m = n_m M_m \\ P_{HM1} = n_{HM1} M_{HM1} \end{cases} \tag{15}$$

The hydraulic power diversion ratio ρ_{HM1} model is obtained for the *HM1* sector by associating Formulas (12), (14) and (15):

$$\rho_{HM1} = \frac{p_m}{p_{HM1}} = \left| \frac{\varepsilon k_2 (i_1 i_2 + \varepsilon k_1)}{(i_1 i_2)^2 (1 + k_1)(1 - k_2)} \right| \tag{16}$$

Similarly, the hydraulic power split ratio ρ_{HM2} model can be obtained for the *HM2* section:

$$\rho_{HM2} = \frac{p_m}{p_{HM2}} = \left| \frac{\varepsilon k_2 [\varepsilon k_2 (1 + k_1) + (1 - k_2)(i_1 i_2 + \varepsilon k_1)]}{(i_1 i_2)^2 (1 + k_1)} \right| \tag{17}$$

From the above hydraulic power shunt ratio model, when $\varepsilon = 1$, $\begin{cases} \rho_{HM1} = 0.167 \\ \rho_{HM2} = 0.5 \end{cases}$; when $\varepsilon = 0$, $\begin{cases} \rho_{HM1} = 0 \\ \rho_{HM2} = 0 \end{cases}$; when $\varepsilon = -1$, $\begin{cases} \rho_{HM1} = 0.056 \\ \rho_{HM2} = 1.5 \end{cases}$.

The variation characteristics of the HMT power shunt ratio of the cotton picker are obtained as shown in Figure 5.

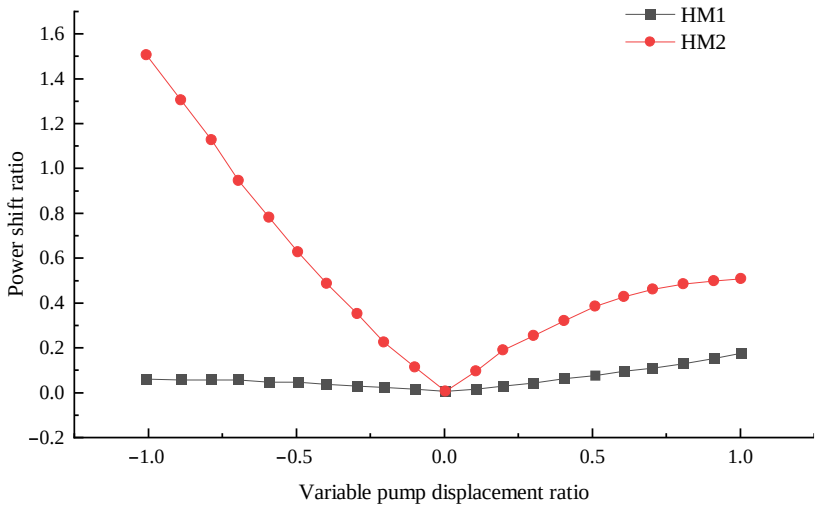

Figure 5. Hydraulic power split ratio of each section of HMT.

Based on Figure 5, it is evident that the split ratio of the cotton picker HMT in the low-speed *HM1* forward section and the high-speed *HM2* forward section exhibits continuous variation. When the pump displacement ratio ε is at 0, the split coefficient ρ reaches its minimum value. Under these circumstances, the hydraulic power is zero, and the hydraulic power flow does not contribute to the converging process of the planetary gear system, resulting in the highest system efficiency. According to the characteristic curve of the hydraulic power diversion ratio in each section of HMT, different variable pump displacement ratios can be selected to meet the different requirements of the cotton picker traveling system in the harvesting conditions and road transport conditions, to improve the efficiency of HMT.

2.5. HMT Bench Test

The measurement and control principle of the HMT test bench of the cotton picker is shown in Figure 6. The NI LabVIEW 2020 software is used to develop the human–machine interaction interface, the conditional structure is used to control variable pumps and motors, and the lower machine TCU adopts the sequential structure to collect data and control the equipment. And the test site is the hydraulic hall of the School of Mechanical and Electrical Engineering of Shihezi University. The schematic diagram of the test rig is shown in Figure 7, and the main component parameters of the HMT test are shown in Table 4.

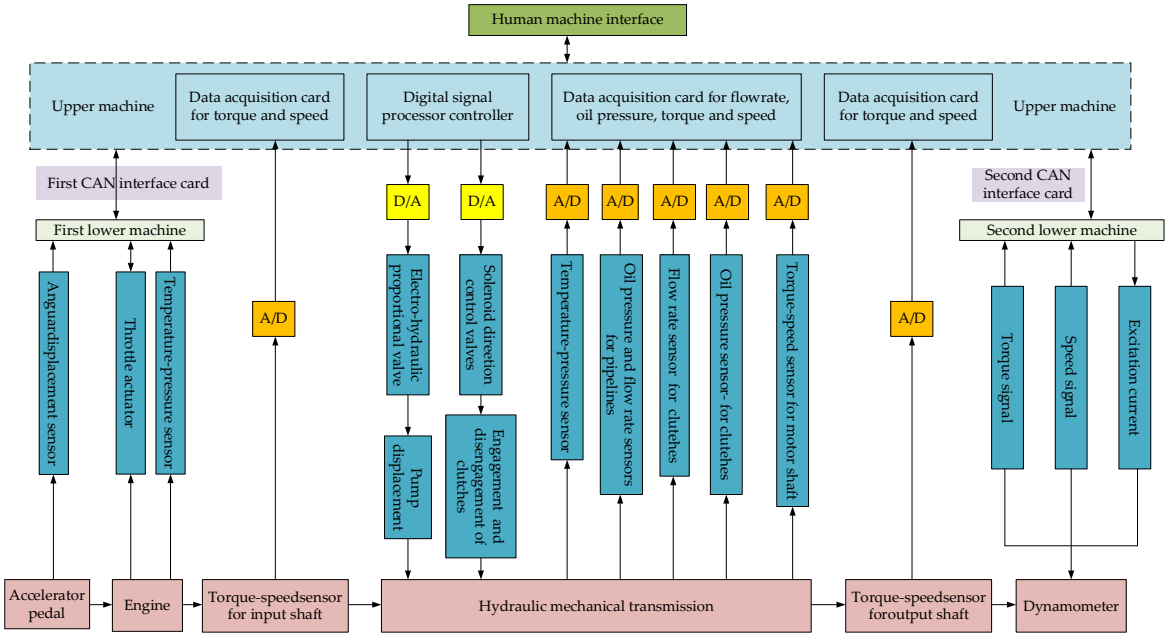

Figure 6. HMT test bench measurement and control principle.

Table 4. Main component parameters of HMT test bench.

Number	Code	Name	Quantity	Specification
1	4045HYC11	Engine	1	2400 rpm; 130 kW
2	ZJ 2000 series	Speed and torque sensors	2	0~3000 rpm; 2000 N·
3	HPV series	Pump	1	54.7 cc/rev
4	HPV series	Motor	1	51.3 cc/rev
5	3144E	Solenoid relief valves	3	3~3.5 V
6	YW Series	Pressure sensors	4	10 MPa
7	DG series	Flow Meters	6	M20 × 1.5
8	DN25 Series	Turbine Flow Sensor	2	170 L/min
9	LWGY-DN15	Magnetic particle brakes	2	0.6~10 m^3/h

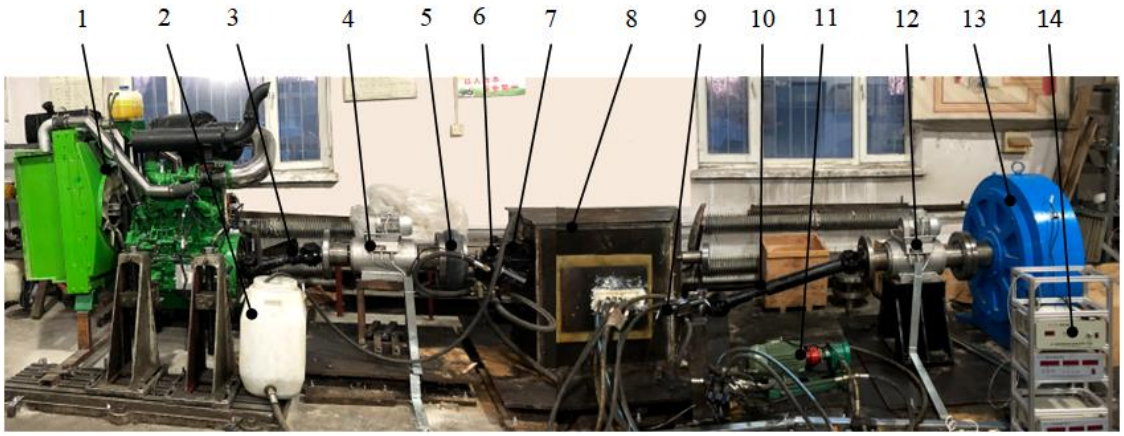

Figure 7. HMT test bench: 1—engine; 2—fuel tank; 3—universal joint coupling; 4—speed and torque sensor; 5—flexible coupling; 6—variable pump; 7—hydraulic motor; 8—HMT; 9—solenoid valve; 10—auxiliary pump; 11—universal joint coupling; 12—speed and torque sensor; 13—magnetic particle brake; 14—data acquisition instrument.

2.5.1. Speed Ratio Continuity Test

No-load and loading tests were carried out on the output speed of the cotton picker HMT at different engine speeds to analyze and verify the speed ratio continuity characteristics of the cotton picker HMT.

Initially, the control system was interfaced with the controller via LabVIEW to modulate the electronic throttle valve of the engine, thereby regulating its output speed for stability. Subsequently, the displacement ratio of the controlled hydraulic pump was adjusted to facilitate continuous acceleration of the cotton picker's HMT. Furthermore, the engagement and disengagement of the clutch were managed by transmitting control signals to the electromagnetic directional control valve, thereby accomplishing the acceleration phase of the HMT during segment shifts.

The procedural stages were as follows: Initially, from 0 to 5 s, the displacement ratio of the controlled hydraulic pump was incrementally adjusted from 0 to −1, while simultaneously fine-tuning the electronic throttle valve to ensure the engine promptly attained the target speed, thereby achieving a seamless startup. Following this, from 5 to 15 s, after the variable pump's displacement ratio transitioned from −1 to 1, the engine reached the target speed, enabling the acceleration of the gearbox within the *HM1* section. During this period, the bidirectional clutch C1 was engaged on the right, and bidirectional clutch C2 was engaged on the left.

Subsequently, at 15 s, the clutch engagement and disengagement were manipulated to facilitate the acceleration of the cotton picker HMT into the next section, with clutch C2 being engaged on the left. Thereafter, from 15 to 30 s, the displacement ratio of the variable pump was altered from 1 to −1, which allowed for the acceleration of the gearbox in the *HM2* zone. At this juncture, bidirectional clutch C1 was engaged on the left, and bidirectional clutch C2 was engaged on the right. Finally, from 30 to 40 s, the pump displacement ratio was maintained at −1 to record the output speed of the cotton picker HMT.

During the no-load test, we set the electronic throttle opening so that the engine's constant speed output target was 600 rpm, 1200 rpm, 1800 rpm, and 2400 rpm, and the test was carried out sequentially at the four target speeds. During the loading test, the electronic throttle opening was set so that the engine constant speed output target was 1200 rpm, 1800 rpm, and the constant loading test was carried out sequentially at 2 target speeds, with the loading torque sizes of 100 N·m, 150 N·m, and 200 N·m, respectively. To prevent random errors, 5 tests were carried out at each engine speed, and the average value was taken as the final data with simple linear processing.

2.5.2. Shift Smoothness Test

The specific requirements of good smoothness of the section change need to ensure a smooth speed trend first. Secondly, there is no excessive instantaneous acceleration (deceleration) speed, to improve the comfort of vehicle personnel [25]. The evaluation indexes of smoothness are speed drop, dynamic load coefficient, shift jerk, and slip work.

(1) Speed drop

In the process of transmission segment change, the clutches must be engaged one after another because the drive shaft cannot engage the output speeds of the two clutches at the same time, and in the process of the successive engagement of the clutches, the phenomenon of speed drop occurs.

At this time, the output shaft mechanical path is disconnected, and the hydraulic pressure can provide HMT speed, defining the difference between the steady-state output speed n_s of the HMT and the minimum output speed n_{min} as the speed drop γ of the HMT.

$$\gamma = |n_{\min} - n_s| \tag{18}$$

(2) Dynamic load factor

The torque transmitted by the clutch is converted from dynamic slip torque to static slip torque due to load fluctuation during the transmission shift, and the dynamic load coefficient δ responds to the vigor of this process.

$$\delta = \left| \frac{T_{\max}}{T_s} \right| \tag{19}$$

In Formula (19), T_{max} is the maximum output torque value of the HMT, N·m; T_s is the steady-state output torque value of HMT, N·m.

(3) Shift jerk

The rate of change in instantaneous acceleration of the vehicle during the transmission shift is expressed as the shift jerk J (m/s^3), which is the 2nd order derivative of the vehicle traveling speed to time:

$$J = \frac{da}{dt} = \frac{d^2v}{dt^2} = \frac{r_d(M_e i_a)}{I i_b dt} \tag{20}$$

In Formula (20), I is the output shaft-associated part of inertia, m/s^3; i_a is the transmission ratio; i_b is the drive axle ratio; M_e is the engine torque, N·m; r_d is the wheel radius, m; v is the vehicle traveling speed, m/s; t is the time, s; a is the vehicle acceleration, m/s^2.

(4) Slip work

In the process of clutch segment switching, which is the main slippery state, the clutch oil-filling piston overcomes the spring force to carry out work and move, and in the process of oil unloading due to the force of the spring, the piston begins to return to the position [25]. The work carried out in this process is the slip work W_f (J), which is expressed as

$$W_f = \int_{t_0}^{t_t} P_f dt = \int_{t_0}^{t_t} T_f |\triangle w| dt \tag{21}$$

In Formula (21), t_0 is the start time of the slipping process; t_t is the end time of the slipping process; T_f is the clutch torque, N·m; and P_f is the clutch slipping power, kW.

Based on the above evaluation indexes, the HMT shift smoothness test was carried out with different engine speeds, load torque, main oil pressure, and governor valve flow size as single factors to obtain the influence law of the shift process.

In examining the impact of a constant engine speed on the HMT transition, the following test parameters were established: engine speeds of 1200, 1800, and 2400 rpm,

with a consistent load torque of 100 N·m, main oil pressure at 3.5 MPa, and a governor valve flow rate of 3.5 L/min.

To assess the influence of load torque on the HMT shift dynamics, the experimental setup included engine speeds of 1200, 1800, and 2400 rpm, while the load torque was varied at 75 N·m, 100 N·m, and 125 N·m, maintaining a main oil pressure of 3.5 MPa and a governor valve flow rate of 3.5 L/min.

When investigating the effect of main oil pressure on the HMT shift process, the test conditions were set with a fixed engine speed of 1800 rpm, a load torque of 100 N·m, and a governor valve flow rate of 3.5 L/min, while the main oil pressure was adjusted to 2.5 MPa, 3.5 MPa, and 4.5 MPa, respectively.

For the study of governor valve flow rate as a single variable affecting the HMT shift process, the experimental conditions were defined as follows: a constant engine speed of 1800 rpm, a load torque of 100 N·m, a main oil pressure of 3.5 MPa, and governor valve flow rates of 2.5 L/min, 3.5 L/min, and 4.5 L/min. The HMT shift was executed precisely at the 14th second during the experimental procedure.

3. Results and Discussion

3.1. Analysis of Speed Ratio Continuity Results

3.1.1. Analysis of Unloading Test Results

From Figure 8, it is evident that under continuous acceleration, the cotton picker HMT transitions from the engine starting phase to the HM1 section, and then from the HM1 section to the HM2 section. Due to the displacement ratio being at its peak during these transitions, a certain impact occurs, but its amplitude is small. When in the engine speed stabilized at 600 rpm, 1200 rpm, 1800 rpm, and 2400 rpm, the final cotton picker HMT output stabilization speed reached 899.7 rpm, 1792 rpm, 2698 rpm, and 3590 rpm, respectively. Particularly when switching from the *HM1* zone to the *HM2* zone, its output speed was 288 rpm, 580 rpm, 922 rpm, and 1186 rpm, respectively, which is in line with the rule of the law of change of equipartition. The HMT speed ratio matching program is continuously controllable, and its speed ratio matching characteristics are in line with the simulation results, and the design is reasonable.

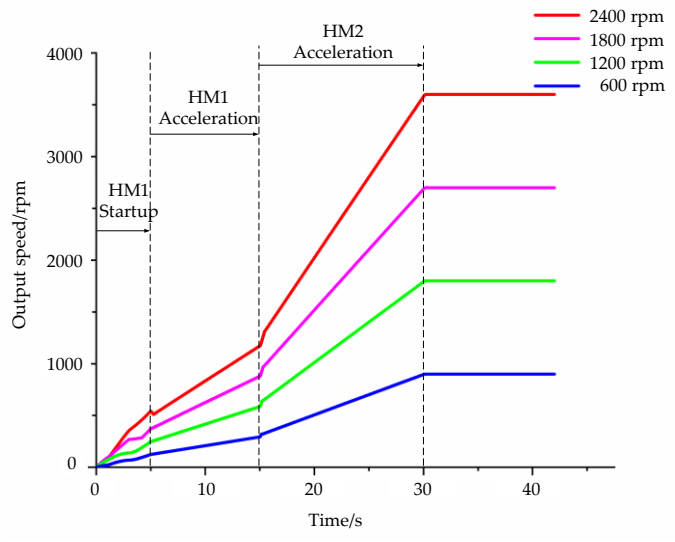

Figure 8. HMT output speed of no-load test.

3.1.2. Analysis of Loading Test Results

From Figure 9, it can be seen that the load torque has a greater impact on the section change process. With the increase in load torque, there is a greater output speed fluctuation at the transition from the *HM1* section to the *HM2* section under the same engine speed. In the *HM2* section, the greater the load torque, the longer the response time required for the

cotton picker HMT to reach the target speed, but the load torque has little impact on the speed ratio of the cotton picker HMT at the transition from the starting stage of the engine to the *HM1* section. The comparison shows that, with the increase in engine speed, the degree of fluctuation of the output speed of the cotton picker HMT under the same load torque condition increases with the increase in the stable output speed of the engine.

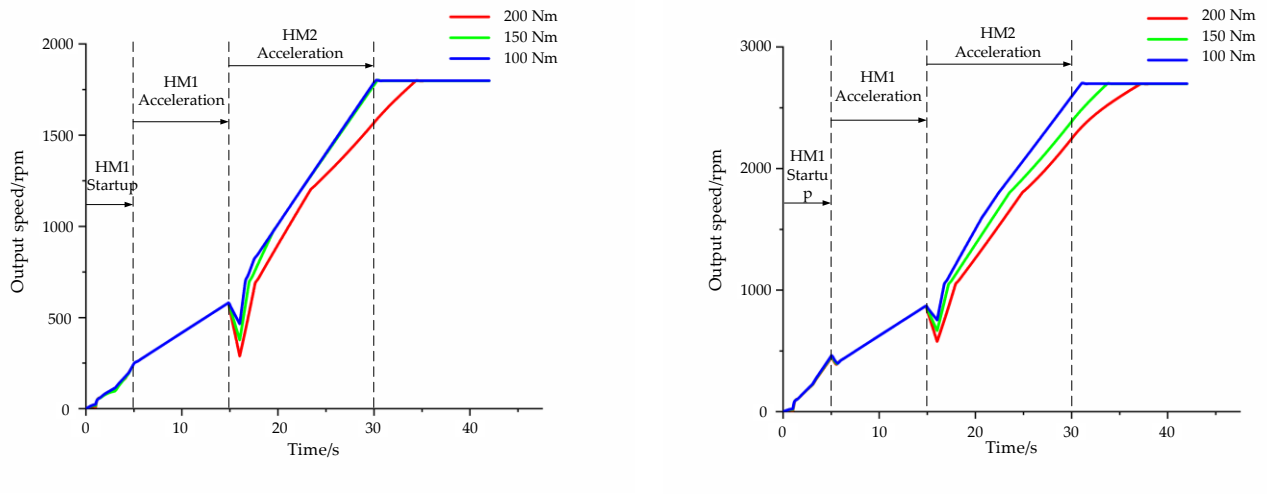

(**a**) 1200 rpm (**b**) 1800 rpm

Figure 9. HMT output speed of loading test.

3.2. HMT Section Change Test

3.2.1. Effects of Different Engine Speeds on the HMT Changeover Process

From the analysis of Figure 10a, it can be seen that the corresponding speed drops are 200.44 rpm, 200.42 rpm, and 200.44 rpm at engine speeds of 1200 rpm, 1800 rpm, and 2400 rpm, respectively, and the speed drops before and after the segment change are the same. Figure 10b shows that the peak value of the HST output torque and the dynamic load factor do not differ much at different constant engine speeds. The dynamic load factor reaches the maximum value of 3.80 at about 15.25 s, and at which time, the maximum output torque is about 380.06 N·m. Figure 10c shows that the maximum jerk at different constant engine speeds occurs at the same time at about 15.15 s, reaching 18.37 $m \cdot s^{-3}$, 18.52 $m \cdot s^{-3}$, 18.61 $m \cdot s^{-3}$, and the maximum jerk is basically in the same range. Figure 10d shows that under different constant engine speeds, the stable slip work of the clutch is 6160.47 J, 6135.15 J, and 6110.85 J, respectively, and different constant engine speeds do not have much effect on the slip work.

3.2.2. The Effect of Different Load Torques on the Segment Change Process

The analysis of Figure 11a shows that when the load torque of the cotton picker HMT is 75 N·m, 100 N·m, and 125 N·m, the speed drop is 126.58 rpm, 200.4 rpm, and 275.35 rpm, respectively; the time required for the output shaft to reach the target rotational speed increases with the increase in the load torque, and the speed drop increases with the increase in the load torque under different load torques. At the same time, the time for the HMT output shaft to reach the target speed increases, and the time to reach the peak value is 15.29 s, 15.40 s, and 15.56 s, respectively. Figure 11b shows that with the continuous increase in load torque, the time for HMT output torque to reach its peak is slightly delayed, but the peak value is the same. The maximum HMT torque reaches 379.47 N·m, 380.06 N·m, and 380.29 N·m at 15.13 s, 15.25 s, and 15.39 s, respectively. The corresponding dynamic load coefficients are 5.06, 3.80, and 3.04, respectively, and the dynamic load coefficients decrease with the increase in load torque. Figure 11c shows that the maximum shift jerk decreases slightly with the increase in load torque, and the impact duration increases slightly with the

increase in load torque. With the increase in load torque, the maximum shift jerk reaches 18.72 m/s^{-3}, 18.52 m/s^{-3}, and 18.30 m/s^{-3}, respectively. Analysis of Figure 11d shows that the stable slip work of the clutch increases with the increasing load torque, which is 2588.69 J, 6135.26 J, and 11,982.56 J, respectively, indicating that the load torque has a significant effect on the slip work.

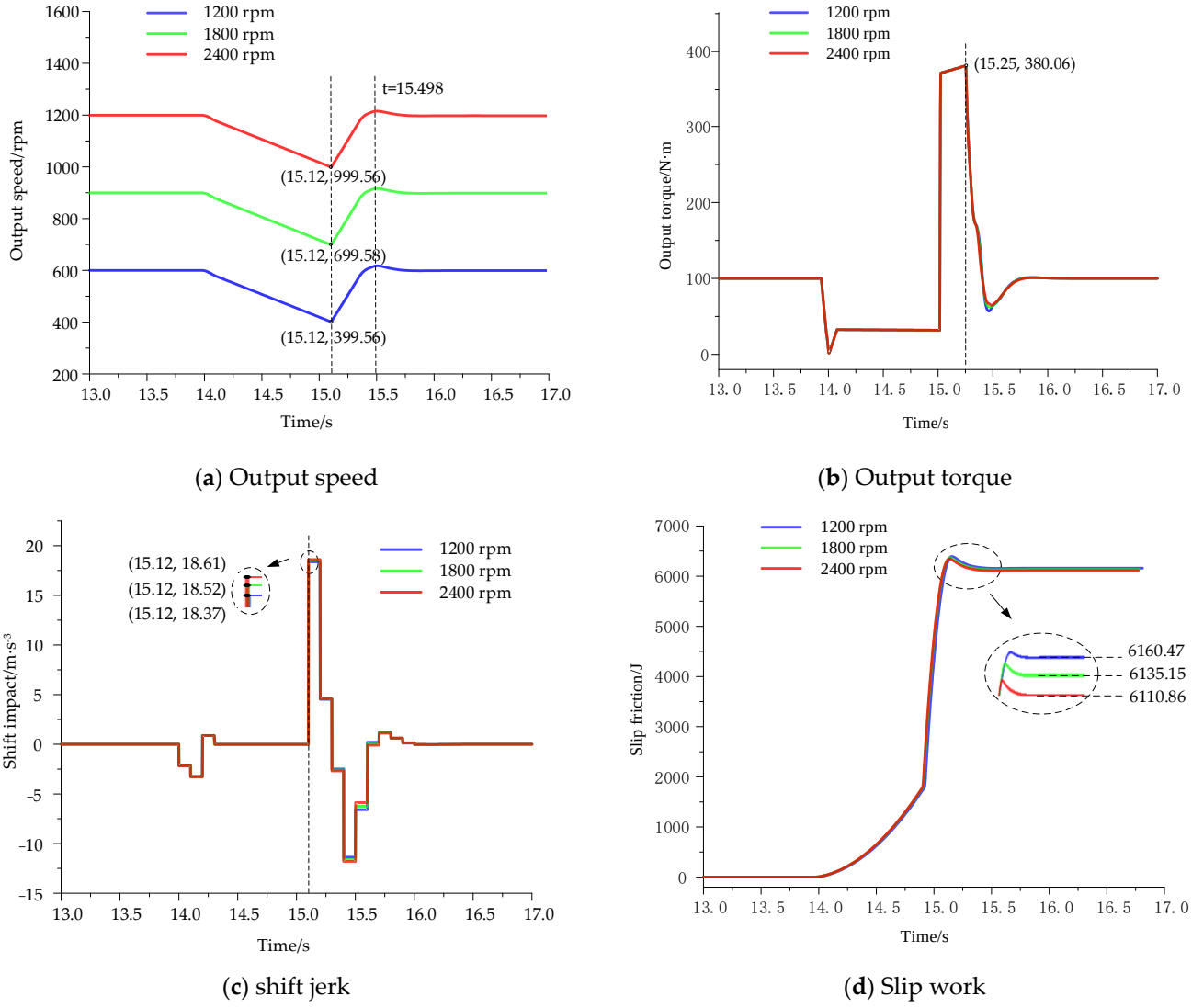

(**a**) Output speed (**b**) Output torque

(**c**) shift jerk (**d**) Slip work

Figure 10. The influence of engine speed on HMT shift.

3.2.3. Effect of Different Main Circuit Oil Pressures on the Changeover Process

According to the analysis of Figure 12a, it can be seen that the speed drop is 212.82 rpm, 198.93 rpm, and 212.25 rpm under the main oil pressure of 2.5 MPa, 3.5 MPa, and 4.5 MPa, respectively. The higher the main oil pressure is, the shorter the time required for the HMT output shaft speed to reach the stable target speed, but there is not much difference in the speed drop. According to Figure 12b, the maximum output torque of the HMT reaches 271.69 N·m, 380.06 N·m, and 487.95 N·m at 15.48 s, 15.25 s, and 15.18 s, respectively. The dynamic load coefficients are 2.72, 3.80, and 4.88, respectively, as the main oil circuit pressure keeps increasing, and the time to reach the peak value decreases with the increase in the main oil circuit pressure. Figure 12c shows that the maximum shift jerk reaches 12.61 m/s^{-3}, 18.53 m/s^{-3}, and 24.34 m/s^{-3} with the increase in the main oil circuit pressure, and occurs at about 15.15 s at the same time. The maximum shift jerk increases with the increase in the main oil circuit pressure, and the jerk duration decreases with the

increase in the main oil circuit pressure. Analysis of Figure 12d shows that as the main oil circuit pressure increases, its clutch stable slipping friction work is 8658.69 J, 6135.26 J, and 6090.5 J, respectively, and the slipping friction work decreases with the increase in the main oil circuit pressure, but the impact is weakened when the main oil circuit pressure increases to a certain threshold value.

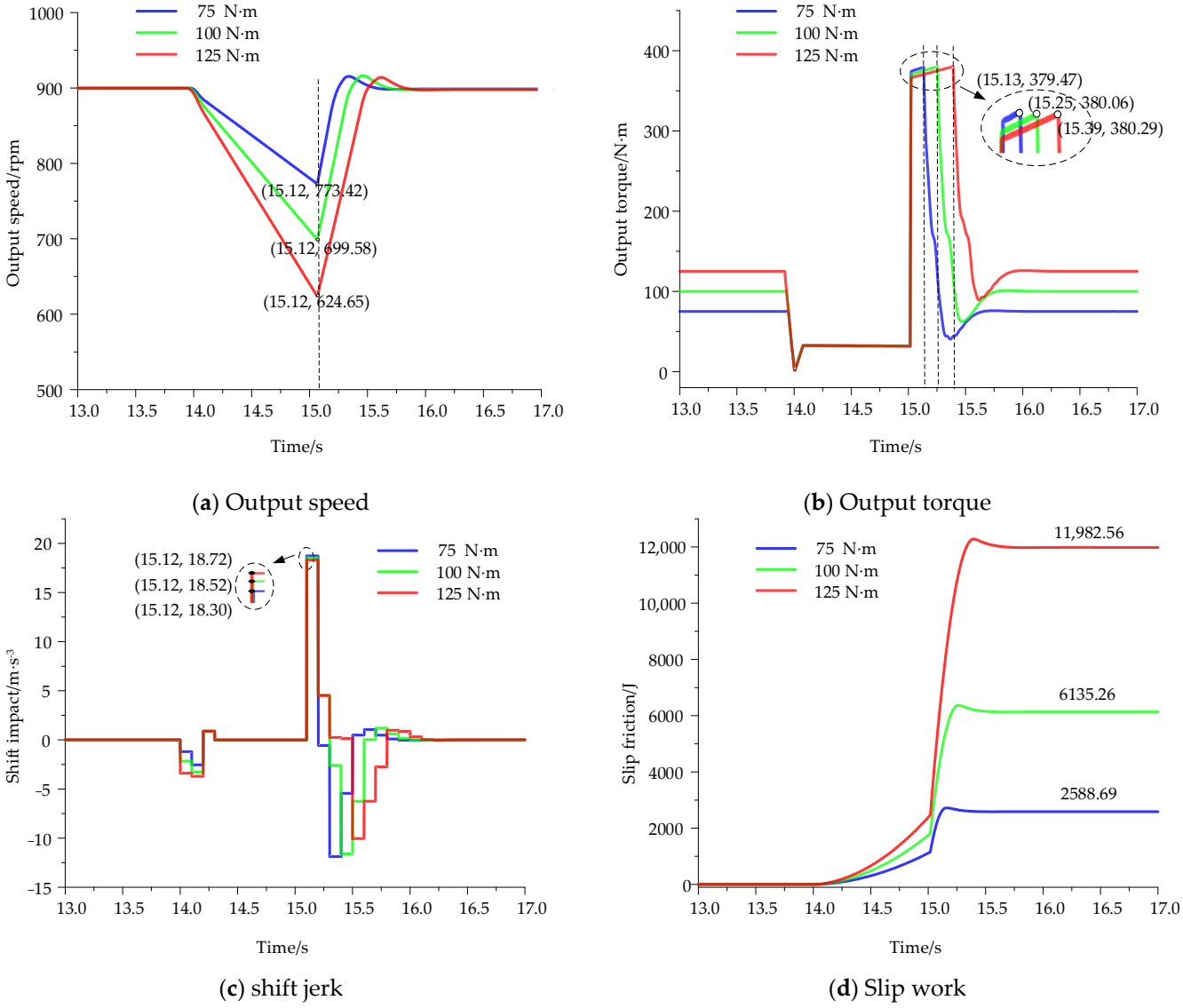

(**a**) Output speed (**b**) Output torque

(**c**) shift jerk (**d**) Slip work

Figure 11. The influence of load torque on HMT shift.

3.2.4. Effect of Different Regulator Valve Flow Rates on the Changeover Process

The effect of HMT on the speed drop of the output shaft of the HMT at different speed control valve flow rates is shown in Figure 13a. The result shows that different speed control valve flow rates have a greater effect on the change in the speed drop of the output shaft, and as the speed control valve flow rate continues to increase, the speed drop of the output shaft decreases, and the speed drop is 290.4 rpm, 198.93 rpm, and 169.5 rpm, respectively, which corresponds to the arrival time at the peak of 15.96 s, 15.40 s, and 15.13 s respectively, and the time for the output shaft speed to reach the stable target speed is shortened with the increase in the governor valve flow rate. The effect of HMT on the dynamic load factor at different governor valve flow rates is shown in Figure 13b. The result shows that under different flow rates of the speed regulating valve, as the flow rate of the speed regulating valve continues to increase, the maximum output torque of HMT

reaches 380.28 N·m, 380.06 N·m, and 377.39 N·m at 15.79 s, 15.25 s, and 14.92 s, respectively, and the corresponding dynamic load coefficients are 3.80, 3.80, and 3.77, respectively. The peak time of HMT's maximum output torque decreases with the increase in the main oil pressure, and the dynamic load coefficient is basically not affected. The effect of HMT at different speed control valve flow rates on the shift jerk is shown in Figure 13c. The result shows that the maximum impact reaches 16.034 m/s^{-3}, 18.528 m/s^{-3}, and 21.053 m/s^{-3} at 15.51 s, 15.20 s, and 14.91 s, respectively. With the increase in the flow rate of the speed regulating valve, the maximum impact time is advanced, and the maximum impact degree is gradually increased. The effect of HMT on slip work at different speed control valve flow rates is shown in Figure 13d. The result shows that the higher the flow rate of the speed regulating valve, the shorter the time required for the sliding work to reach the stable value. The stable sliding work of the clutch is 13,580.29 J, 6135.26 J, and 4322.35 J respectively, and with the continuous increase in the flow rate of the speed regulating valve, the stable value of the sliding work gradually decreases, indicating that the flow rate of the speed regulating valve has an obvious influence on the sliding work.

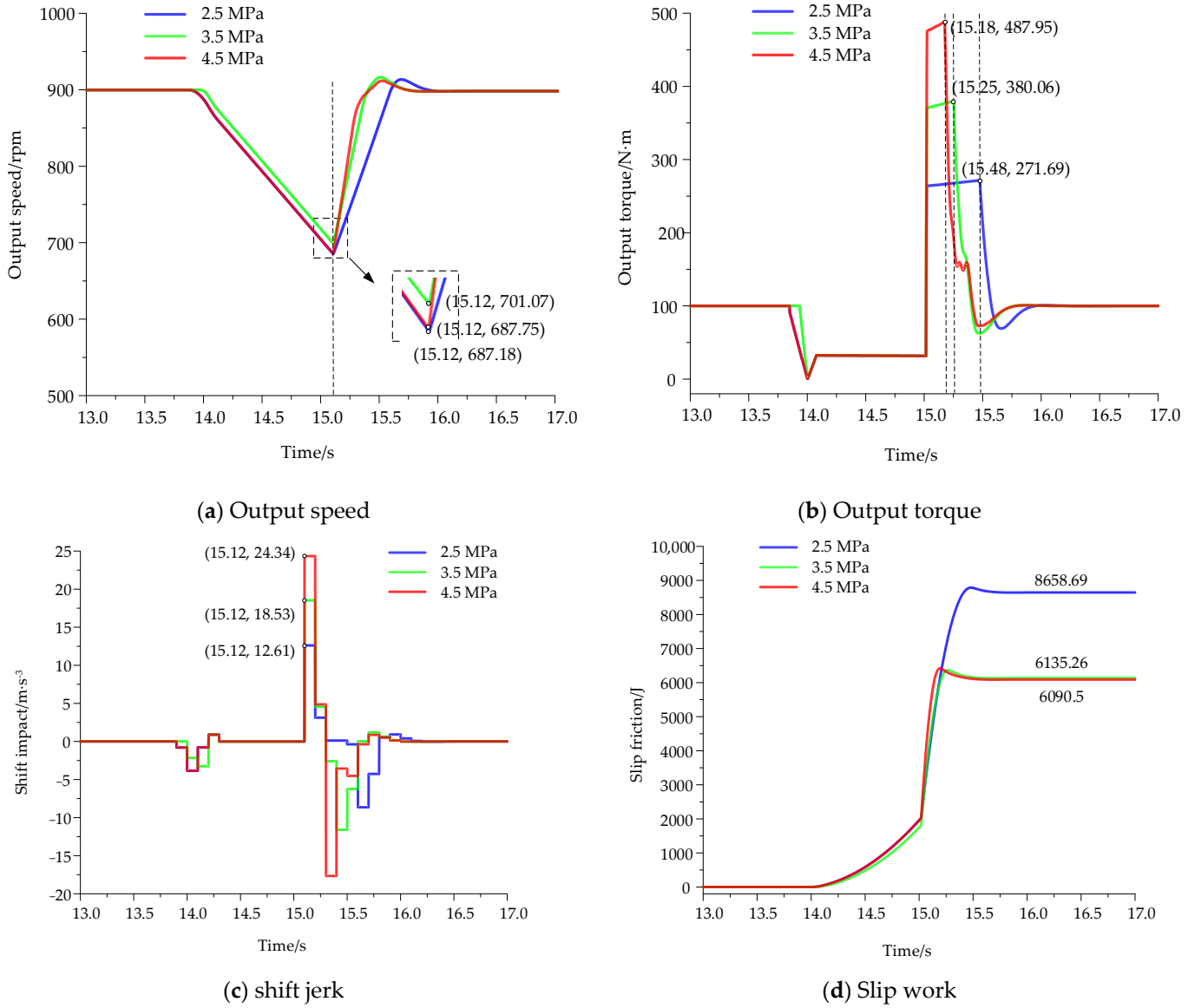

Figure 12. The influence of oil pressure on HMT shift.

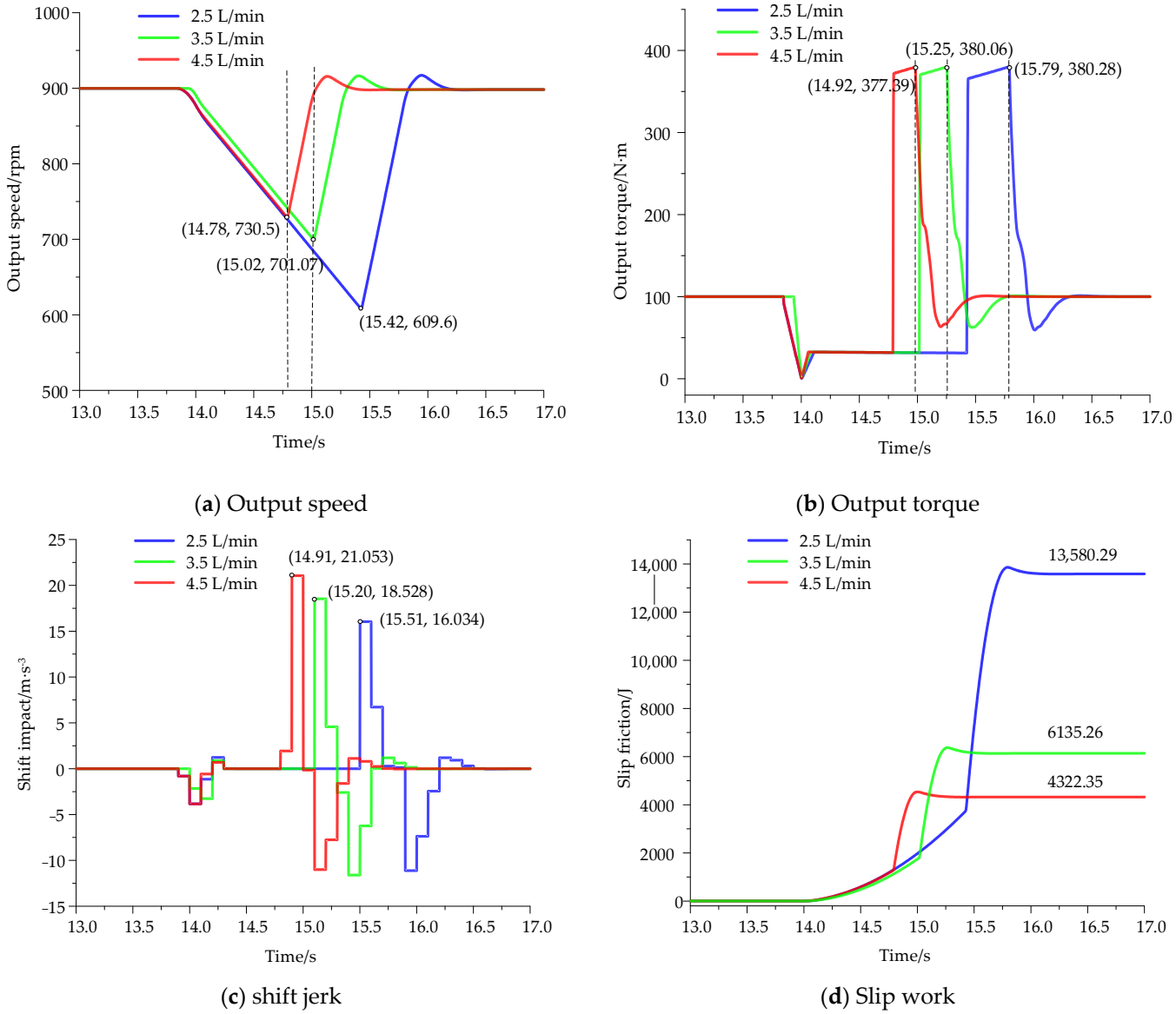

(**a**) Output speed (**b**) Output torque

(**c**) shift jerk (**d**) Slip work

Figure 13. The influence of oil circuit flow on HMT shift.

In summary, the experimental protocol conducted on the test rig for the continuous speed ratio matching of the cotton picker's hydro-mechanical transmission (HMT) confirmed the system's capability for continuous and controllable speed ratio adjustment, with the output rotational speed adhering to a proportional variation law. The segment shifting experiments of the HMT revealed that the load torque plays a critical role in the transition process. An increase in load torque corresponds to enhanced fluctuations in the output rotational speed during the shift from the *HM1* to *HM2* segment, thereby lengthening the response time necessary for the HMT to achieve the target rotational speed. Variations in the stable output rotational speed of the engine exert minimal influence on the assessment criteria for HMT segment shifts. The main oil circuit flow rate has a significant impact on the speed reduction, whereas the load torque exhibits an extremely pronounced effect. Both the load torque and the main oil circuit pressure are highly influential factors affecting the dynamic load coefficient. Furthermore, the load torque significantly influences the degree of shock and has a marked impact on the friction work associated with clutch engagement.

4. Conclusions

(1) The analysis of the HMT speed ratio matching scheme for the cotton picker, including the speed ratio matching logic and specific matching parameters, has confirmed the transmission ratio, output speed, output torque, and power split ratio characteristics through calculation. The cotton picker operates within a speed range of 3–10 km/h in the *HM1* forward and backward low-speed sections and 10–30 km/h in the *HM2* forward section, which is suitable for both field harvesting and road transportation states.

(2) Continuous tests on the test bench have verified that the HMT speed ratio of the cotton picker is continuously controllable, with the output speed adhering to the law of proportional change. However, the load torque significantly affects the transition process between different sections, particularly from *HM1* to *HM2*, where an increase in load torque leads to greater fluctuations in output speed and a longer response time to reach the target speed.

(3) The stable output speed of different engines has a minimal impact on the evaluation indices of each HMT stage. However, the flow rate of the main oil circuit and load torque are crucial factors affecting speed drop, dynamic load coefficient, impact degree, and slip friction work.

Therefore, to enhance the quality of HMT section transitions in cotton pickers, it is imperative to prioritize the stabilization of load torque during segment shifts. Subsequently, optimization of the main oil circuit's pressure and flow rate, under stable load torque conditions, is crucial. This approach can refine the HMT's section transition quality. The findings of this study lay the groundwork for further investigation into optimizing shift processes, enhancing shift smoothness, and designing dynamic control systems. Concurrently, the research offers theoretical support for the development and design of cotton picker gearboxes, as well as for the transmission characteristics and experimental studies of off-road vehicle transmissions.

Author Contributions: Conceptualization, H.C., M.W. and X.N.; methodology, H.C. and M.W.; software, H.C., Y.L. and X.M.; validation, M.W., B.Z. and W.C.; formal analysis, H.H. and M.W.; investigation, X.N. and X.M.; resources, X.N.; data curation, Y.L.; writing—original draft preparation, H.C.; writing—review and editing, H.C. and M.W.; visualization, Y.W.; supervision, X.N. and W.C.; project administration, W.C.; funding acquisition, X.N. All authors have read and agreed to the published version of the manuscript.

Funding: This research was funded by the National Natural Science Foundation of China, grant number 51665051, and supported by Bingtuan Science and Technology Program, grant number 2022AA001.

Institutional Review Board Statement: Not applicable.

Data Availability Statement: All relevant data presented in the article are kept at the request of the institution and are therefore not available online. However, all data used in this manuscript are available from the corresponding authors.

Acknowledgments: Thanks to the National Natural Science Foundation of China (grant number: 51665051) and Xinjiang Production and Construction Corps major financial science and technology projects for funding. Thanks to Xinjiang Swan for providing cotton-picking machines and helping with trials. In addition, thanks to the anonymous reviewers for providing critical comments and suggestions for improving the manuscript.

Conflicts of Interest: The authors declare no conflicts of interest.

References

1. Wu, Q.; Zhu, J. Factor substitution and regional differences of cotton production in China. *J. China Agric. Univ.* **2019**, *29*, 221–230.
2. Zhang, R.; Chen, Y.; Zhao, D. Development status and suggestions of the cotton industry in Xinjiang. *J. Smart Agric.* **2023**, *3*, 5.
3. Zhao, Y.; Chen, X. Problems and prospects of high quality cotton production in China. *J. Tarim Univ.* **2023**, *35*, 8.

4. Mishra, P.K.; Sharma, A.; Prakash, A. Current research and development in cotton harvesters: A review with application to Indian cotton production systems. *Heliyon* **2023**, *9*, e16124. [CrossRef] [PubMed]
5. Yuan, Y.; Bai, S.; Niu, K.; Zhou, L.; Zhao, B.; Wei, L.; Liu, L. Research progress in the key technologies and equipment for cotton planting mechanization. *Trans. Chin. Soc. Agric. Eng.* **2023**, *39*, 11.
6. Li, H.; Fu, X.; Wang, H.; Zhang, H.; Gu, Y.; Du, X.; Tao, Y.; Li, J. Research on the Wear Characteristics of the Hook Teeth of Cotton Pickers. *Coatings* **2022**, *12*, 762. [CrossRef]
7. Niu, G.; Li, B.; Liu, Y.; Li, Y.; Wang, T.; Wang, S. Development and research status of cotton picker in China. *J. Chin. Agric. Mech.* **2020**, *41*, 7.
8. Chen, T.; Zhang, H.; Wang, L.; Wang, Y.; Zhang, L.; Li, X. Research and experiment on movement characteristies ofpicking mechanism of horizontal picking cotton picker. *J. Chin. Agric. Mech.* **2020**, *41*, 19–25. [CrossRef]
9. He, X.; Gong, L.; Miao, Z.; Miao, Z.; Han, K.; Hao, F.; Han, Z. Automatic alignment control method of cotton picker based on parallel trajectory navigation. *J. Trans. Chin. Soc. Agric. Mach.* **2024**, *55*, 34–41.
10. Miao, Z.; Li, C.; Han, K.; Hao, F.; Han, Z.; Zeng, L. Optimal Control Algorithm and Experiment of Working Speed of Cotton-picking Machine Based on Fuzzy PID. *Trans. Chin. Soc. Agric. Mach.* **2015**, *46*, 9–14+27.
11. Zhu, C.; Zhang, H.; Wang, W.; Li, K.; Liu, W. Robust control of hydraulic tracked vehicle drive system based on quantitative feedback theory. *Int. J. Distrib. Sens. Netw.* **2020**, *16*, 155014772090783. [CrossRef]
12. Zhang, G.; Wang, K.; Xiao, M.; Tang, M. Research on Steady-state Transmission Efficiency of HMCVT Based on Hydraulic Mechanical Transmission Torque Ratio. *J. Trans. Chin. Soc. Agric. Mach.* **2023**, *201*, 533–541.
13. Cheng, Z.; Lu, Z. System response modeling of HMCVT for tractors and the comparative research on system identification methods. *Comput. Electron. Agric.* **2022**, *202*, 107386. [CrossRef]
14. Mattetti, M.; Michielan, E.; Mantovani, G.; Varani, M. Objective evaluation of gearshift process of agricultural tractors. *Biosyst. Eng.* **2022**, *224*, 324–335. [CrossRef]
15. Baek, S.-M.; Kim, W.-S.; Kim, Y.-S.; Baek, S.-Y.; Kim, Y.-J. Development of a Simulation Model for HMT of a 50 kW Class Agricultural Tractor. *Appl. Sci.* **2020**, *10*, 4064. [CrossRef]
16. Park, Y.-J.; Kim, S.-C.; Kim, J.-G. Analysis and verification of power transmission characteristics of the hydromechanical transmission for agricultural tractors. *J. Mech. Sci. Technol.* **2016**, *30*, 5063–5072. [CrossRef]
17. Ahn, H.-J.; Park, Y.-J.; Kim, S.-C.; Choi, C. Theoretical Calculations and Experimental Studies of Power Loss in Dual-Clutch Transmission of Agricultural Tractors. *Agriculture* **2023**, *13*, 1225. [CrossRef]
18. Wan Soo, K.; Yeon Soo, K.; Taek Jin, K.; Seong Un, P.; Yong, C.; Il Su, C.; Young Keun, K.; Yong Joo, K. Analysis of Power Requirement of 78 kW Class Agricultural Tractor According to the Major Field Operation. *Trans. Korean Soc. Mech. Eng. A* **2019**, *43*, 911–922.
19. Siddique, M.A.A.; Baek, S.-M.; Baek, S.-Y.; Kim, Y.-J.; Lim, R.-G. Development, Validation, and Evaluation of Partial PST Tractor Simulation Model for Different Engine Modes during Field Operations. *Agriculture* **2023**, *13*, 44. [CrossRef]
20. İnce, E.; Güler, M.A. Design and Analysis of a Novel Power-Split Infinitely Variable Power Transmission System. *J. Mech. Des.* **2019**, *141*, 54501. [CrossRef]
21. Chen, T.; Zhang, H.; Wang, L.; Zhang, L.; Wang, J.; Li, J.; Gu, Y. Optimization and experiments of picking head transmission system of horizontal spindle type cotton picker. *Trans. Chin. Soc. Agric. Eng.* **2020**, *36*, 18–26.
22. Liu, C.; Hu, Z.; Yang, B.; Liu, X. Design and Finite Element Analysis of Travelling Transmission of Six-row Cotton Picking and Packing Machine. *J. Tract. Agric. Transp.* **2024**, *51*, 25–29.
23. Wang, X.; Huang, K.; Huang, J.; Wang, H.; Gong, P. Development and experiment of 4MZ-4 Self-propelled box type cotton picker. *J. Xinjiang Agric. Mech.* **2024**, *2*, 32–34+54.
24. Chen, W.; Cao, Y.; Ni, X.; Han, S.; Wang, G.; Xiao, M. Study on transmission characteristics of hydrostatic power split CVT of cotton picker. *J. Chin. Agric. Mech.* **2020**, *41*, 7. [CrossRef]
25. Chen, W.; Xu, Z.; Wu, Y.; Zhao, Y.; Wang, G.; Xiao, M. Analysis of the shift quality of a hydrostatic power split continuously variable cotton picker. *Mech. Sci.* **2021**, *12*, 589–601. [CrossRef]
26. Ni, X.; Bao, M. Dynamic Test of Hydro Mechanical Composite Transmission for Cotton Picker. *J. Beijing Inst. Technol.* **2020**, *29*, 366–378.
27. Bao, M.; Ni, X.; Zhao, X.; Li, S. Research on the HMCVT gear shifting smoothness of the four-speed self-propelled cotton picker. *Mech. Sci.* **2020**, *11*, 267–283. [CrossRef]
28. Zhong, C.; Ni, X.; Han, S.; Zhao, X.; Li, S.; Wei, X. Design and Test of Power Shift Driving Transmission System of Cotton Picker. *Mach. Tool Hydraul.* **2022**, *10*, 19.